Cement & Concrete Composites 37 (2013) 119–125

Contents lists available at SciVerse ScienceDirect

Cement & Concrete Composites

journal homepage: www.elsevier.com/locate/cemconcomp

Effect of sustained tensile loading on SHCC crack widths

William P. Boshoff *, Christo J. Adendorff

Civil Engineering Department, Stellenbosch University, Private Bag X1, Stellenbosch 7602, South Africa

ARTICLE INFO

Article history:
Received 19 April 2012
Received in revised form 29 November 2012
Accepted 30 November 2012
Available online 8 December 2012

Keywords:
Creep
SHCC
Cracking
Shrinkage
Fibres
Tensile

ABSTRACT

Strain Hardening Cementitious Composites (SHCCs) exhibit multiple cracking when subjected to tensile loading and can achieve a strain capacity of more than 4% while resisting the full tensile load. Sustained tensile loading (creep) tests were performed to determine the time-dependant cracking behaviour of SHCC. The sustained load levels ranged from 40% to 80% of the ultimate tensile resistance. In this paper the crack widths during sustained tensile loading of SHCC were quantified. It was found that the average crack widths are not significantly dependant on the level of the creep load. The average crack widths were however found to increase significantly from around 70 μm to more than 200 μm after 7 days of sustained loading, even at a load of less than 50% of the ultimate tensile strength.

1. Introduction

Strain Hardening Cementitious Composites (SHCCs) are a type of the High Performance Fibre Reinforced Cementitious Composites (HPFRCCs) and exhibit pseudo strain hardening during tensile loading. SHCC contain randomly distributed short fibres, normally at a dosage of not more than 2%. During the strain hardening phase, multiple cracking occurs which results in a tensile strain capacity of more than 4% before localisation takes place [1]. These fine, multiple cracks commonly have crack widths less than 80 μm during quasi-static tensile tests [2].

Due to the formation of these fine cracks, compared to relatively large, localised cracking in conventional concrete, SHCC have been proposed as a promising durable material for structural elements containing steel reinforcement [3]. The small crack widths, compared to larger cracks in conventional concrete, decrease or even eliminate the rate at which chlorides, water or gaseous substances penetrate the material [4,5]. This decrease in corrosive substances can lead to less maintenance of structural elements and an increase in the service life of reinforced concrete (RC) structures. Therefore, the long term behaviour of SHCC needs to be investigated and understood.

Limited publications however exist about the time-dependant behaviour of SHCC, especially the tensile creep behaviour. A number of publications addressed the loading rate-effect of SHCC [6–9] and creep under a compression load [10]. However, Boshoff et al. [11] did investigate the tensile creep of SHCC and identified the three most prominent mechanisms contributing to the macroscopic tensile creep strain of SHCC, namely:

- The creep of the matrix, which is the least prominent. It is well-known that any cementitious composite will creep during sustained loading.
- The time-dependent crack initiation, which is the increase of the number of cracks during sustained tensile loading. Even at loads at as low as 50% of the ultimate capacity, additional cracks could initiate when subjected to a sustained tensile load.
- The time-dependent fibre pull-out, which is the prominent source of the tensile creep of SHCC. This mechanism is the cause of widening of cracks over time and is directly linked to the matrix/fibre interface.

Boshoff et al. [12] did a number of tensile creep tests on notched SHCC specimens and quantified the crack widths. The results showed that during sustained tensile loading of SHCC, the width of the cracks can increase from less than 80 μm to more than 300 μm in only 3 weeks. These samples also gave rise to fewer cracks compared to quasi-static tests, however the cracks were wider. The conclusion was made that SHCC crack widths were not only dependant on the stress level, but also the duration the load is applied. The test specimens were however notched and the crack widths during sustained tensile loading in a uniform section still need to be investigated.

* Corresponding author. Tel./fax: +27 21 808 4947.
E-mail addresses: bboshoff@sun.ac.za (W.P. Boshoff), adendorff@sun.ac.za (C.J. Adendorff).

0958-9465/$ - see front matter © 2012 Elsevier Ltd. All rights reserved.
http://dx.doi.org/10.1016/j.cemconcomp.2012.11.009

The maximum crack width is not the focus of this study as the crack widths need to be quantified using a statistical representation, especially if the crack widths are to be used for determining the durability of SHCC [13,14].

In this paper the crack widths during sustained tensile loading on uniform SHCC sections were quantified. This was done by subjecting SHCC specimens to both uniaxial tensile and tensile creep tests. The crack widths were quantified over time using a digital image correlation system.

2. Experimental framework

The aim of the research presented in this paper is to quantify the crack widths of SHCC during sustained tensile loading using descriptive statistics. A number of tensile creep tests were performed using different load levels in order to ascertain whether the crack patterns differ at different load levels. Shrinkage tests were also performed in order to eliminate the effect of shrinkage from the tensile creep strain. The crack widths were measured using a non-contact optical surface strain measuring system and the method is explain in detail in Section 3.

2.1. Test setup

Dumbbell shaped specimens were used in this study and the dimensions and the gauge length are shown in Fig. 1. The sustained tensile tests were performed with the setup that was designed by Boshoff and van Zijl [1] and is shown in Fig. 2a. This setup consists of a lever arm applying a constant tensile load. Free hanging weights are applied to the cantilevered end of the lever arms as shown in Fig. 2a. Two specimens were connected in series which increases the number of tests that can be performed at one time. This does however have the disadvantage that when a specimen fails, the other specimen connected in series is unloaded. The load was applied by lowering a hydraulic jack slowly which temporarily supported the lever arm. Steel plates tightened with bolts were used to clamp the specimens as shown in Fig. 2b.

The creep strains were measured continuously using 10 mm HBM Linear Variable Differential Transducers (LVDTs) over the 80 mm gauge length. These LVDTs were fixed to an aluminium frame which in turn was fastened to the specimens using small screws. This setup is shown in Fig. 2b and c.

2.2. Specimen preparation

The specific mixing ratio and type of constituents that were used for this SHCC are shown in Table 1. The admixtures, namely the viscosity modification agent (VMA) and high range water reducing admixture, were added to improve the workability of the mix. The fibres were supplied by Kuraray, Japan. Sand with particle size of smaller than 600 μm was used as the aggregate. The mixing procedure is summarised in Fig. 3.

After the material was cast into the dumbbell moulds the specimens were moved to a climate controlled room with a temperature of 23 °C ± 2 °C and a relative humidity of 65 ± 10%. After an hour and a half the specimens were levelled with a trowel in order to ensure a flat and uniform surface. Thereafter, flat steel lids were placed on the moulds to prevent moisture loss. The specimens were allowed to set for 24 h in the moulds in the climate room after which the specimens were demoulded and water cured at 23 °C for a further 13 days. At an age of 14 days the specimens were removed from the water and the surfaces were prepared. This preparation is required for the non-contact surface strain measurement and is explained in detail in Section 3. The specimens were tested within a few hours after the surface preparation.

2.3. Test program

Ten specimens were used for the sustained tensile tests. The specimens were not sealed to prevent evaporation, therefore shrinkage did occur during the creep tests. In order to distinguish between the shrinkage and creep during the tests, three specimens were tested in an unloaded state to quantify the shrinkage strain. The average shrinkage strain development was subtracted from all the tensile creep strain results reported in this paper. It is acknowledged that using this simplistic test arrangement the drying creep cannot be distinguished from the basic creep. Therefore all creep values include both drying and basic creep.

The loading was chosen between 40% and 80% of the ultimate tensile capacity. The ultimate tensile capacity is defined as the average maximum stress resisted during the quasi-static tensile tests which are reported in the following section.

2.4. Quasi-static tensile tests

The quasi-static tensile tests were performed in a Zwick Z250 Universal Materials Testing Machine. The load was measured with a 2 kN HBM load cell and the loading rate was chosen to be 0.08 mm/s between the crossheads which resulted in a failure between 5 and 8 min. The displacement over the 80 mm gauge length was measured using the same method as for the creep tests. The tensile test clamps were designed to allow rotation at the top while it was fixed at the bottom.

A typical strain hardening response was found with reasonably good repetition for the quasi-static tensile tests and is shown in Fig. 4. The stress was calculated by dividing the force by the average cross section area in the gauge area for each specimen.

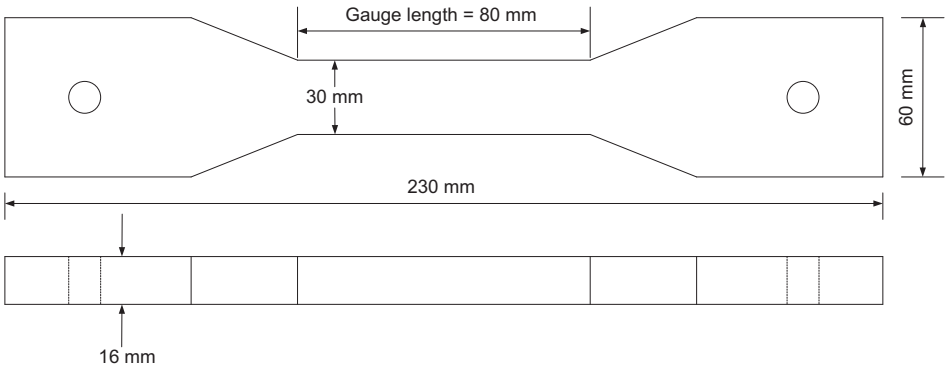

Fig. 1. Dimensions for the dumbbell shaped specimens.

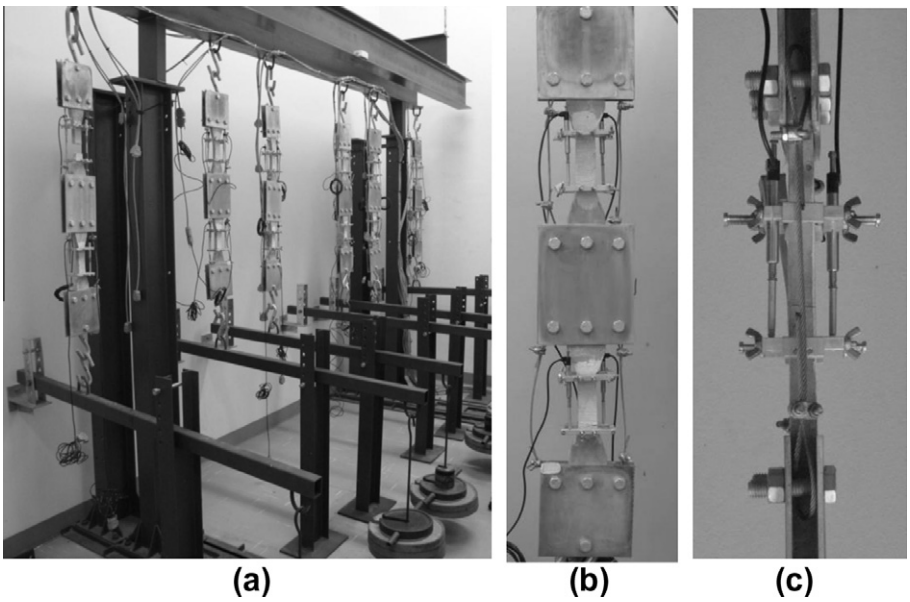

Fig. 2. (a) Tensile creep setup, and (b) and (c), the tensile creep clamps.

Table 1
Constituents and ratio's for the SHCC mix.

Constituents	Ratio/type
Water/binder ratio	0.33
Aggregate/binder ratio	0.46
Water	–
Cement	CEM I 42.5
Fly ash	1:0.85 by mass of cement
Sand	Particle size < 600 μm
Fibre	PVA-RECS 15 Length: 12 mm Diameter: 40 μm 2% by volume
Viscosity modification agent	Chryso Aqua Beton 0.075% of cement
High range water reducing admixture	Chryso Premia 100 0.4% of cement

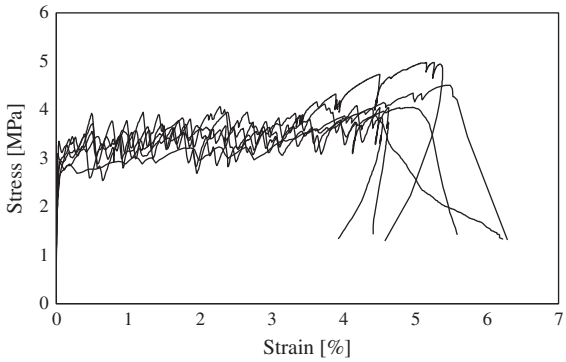

Fig. 4. Uni-axial tensile response for the SHCC test specimens.

The average tensile maximum tensile resistance was 4.26 MPa while, the average strain at failure was 4.70%.

3. The non-contact crack width measuring system

A 3D ARAMIS system with 2 MP cameras supplied by GOM, Germany, was used for measurement of the surface deformations. The system consists of two cameras connected to a PC which takes simultaneous digital images of an object at a specified frequency. The digital images are then analysed by the software in order to determine the surface deformation with regard to a reference image, i.e. the object in an unloaded state.

The surface area is divided into a grid of coordinates with a spacing of 1 mm. The relative displacement of each coordinate is then calculated for each image, i.e. for each step in time.

In order for the software to utilise photogrammetric analysis procedures, a stochastic speckle pattern is required on the surface.

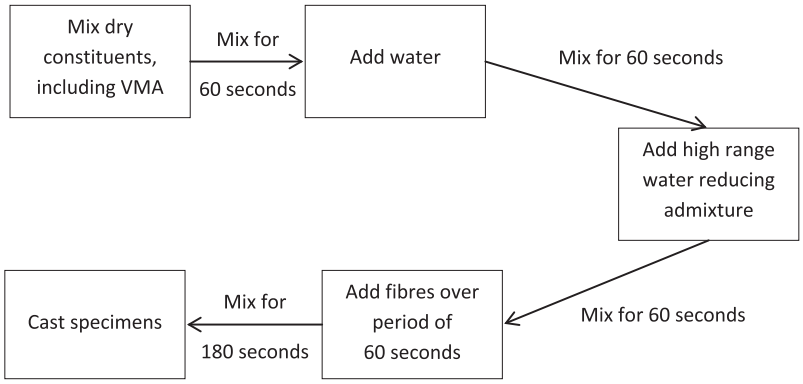

Fig. 3. Mixing procedure.

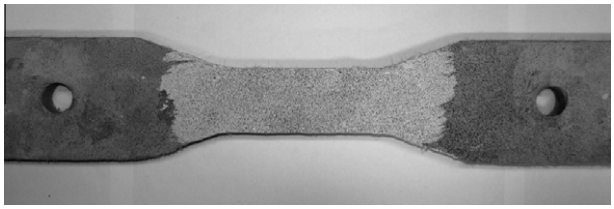

Fig. 5. Typical stochastic pattern on the specimens.

The natural surface of SHCC does not have uniquely definable patterns, therefore the surface had to be prepared.

3.1. Specimen surface preparations

Each specimen was removed from the water prior to testing and all external water was removed using compressed air. The preparation of the surface was done in the gauge area on one side of the specimen, which is the side that was analysed with the aid of the ARAMIS system. A thin layer of ground limestone mixed with water was painted on the surface and allowed to dry. After the drying, normally less than 5 min, black aerosol paint was used to spray a stochastic pattern of black spots on the white limestone layer. A surface prepared specimen is shown in Fig. 5. The preparation was done for all the specimens. The same preparation procedure was also used for the shrinkage specimens so that the drying of these specimens would be consistent with the creep specimens.

3.2. Calculation of crack widths

Before the crack widths at a specific point in time were calculated, the ARAMIS software determined the coordinates in the deformed state. An example of the resulting surface strain contours are shown in Fig. 6. The figure clearly demonstrates the ability of the ARAMIS system to identify the crack positions (represented by the lighter areas) as well as the intensity of the localised strains. The darker areas are uncracked.

The crack widths were determined by evaluating the relative displacement increases between two coordinates in the direction perpendicular to the cracks. A centre line of coordinates were taken for this purpose.

In this study, a crack is defined as a local deformation of more than 15 μm. This implies that when a relative displacement between two coordinates, on the centre line, of more than 15 μm is calculated, it is assumed that a crack formed between the two coordinates. Using this method of crack determination, the number and size of cracks can be calculated with relative ease using the coordinates of the reference stage and the displacement vectors of the coordinates at a specific point in time. The crack widths measured by the ARAMIS system were verified using scaled, high definition photographs.

It is acknowledged that this is a simplistic method of calculating the crack widths. This method will result in errors when two cracks form between two neighbouring coordinates. This method also assumes that all cracks are parallel and do not cross each other. This is however not the case as can be seen in Fig. 6a, but it is assumed that this method will result in accurate enough crack widths for the purpose of this paper.

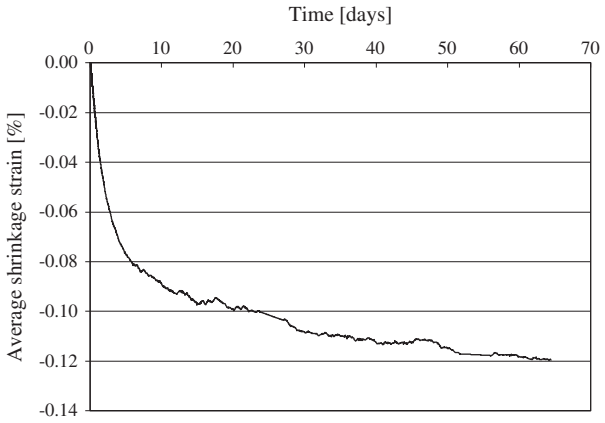

Fig. 7. Average shrinkage strain development.

Table 2
The loading percentages for the 10 tensile creep specimens.

Loading category (%)	Loading percentage of the ultimate stress (%)	Total test time (min)
40–50	40.0	73,330
	49.3	73,330
51–70	58.6	24,740
	60.1	21,920
	60.5	21,920
	61.1	17,460
	64.3	11,840
	65.1	11,840
71–80	74.5	4979
	78.7	4979

4. Experimental results

4.1. Creep deformations

The free shrinkage of three SHCC specimens were measured in order to eliminate the effect of shrinkage of the tensile creep tests. The average shrinkage response is shown in Fig. 7.

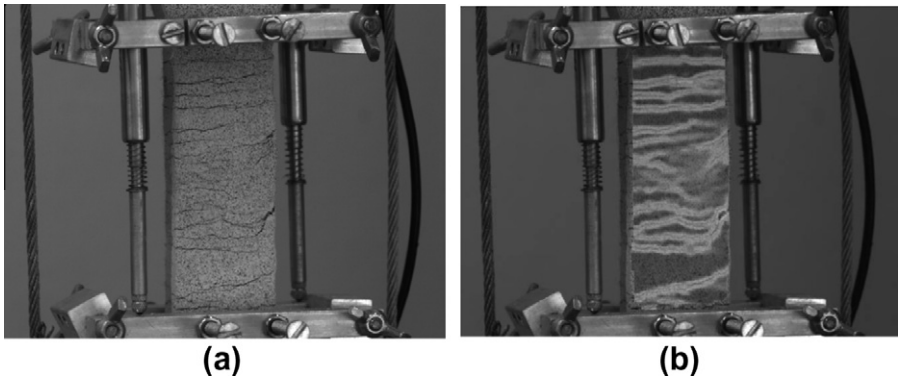

Fig. 6. (a) Typical crack pattern and (b) the visualisation of the crack pattern with surface strain contours.

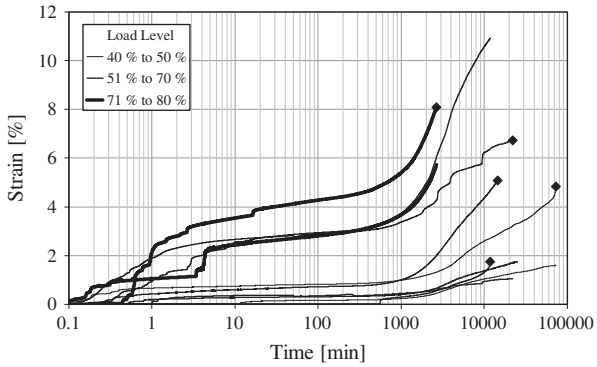

Fig. 8. Tensile creep deformation with a point of failure indicated with a black diamond shaped marker.

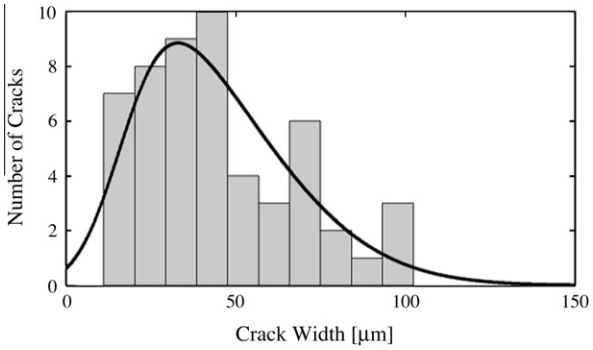

Fig. 10. Histogram of a typical crack pattern with a skewed probability distribution function.

The loading of the 10 specimens varied between 40% and 80% of the ultimate resistance determined during the quasi-static tensile tests. The actual load levels applied are summarised in Table 2. For the simplification of the presentation of the results, the specimens were divided into three categories according to the loading percentage. The three categories are 40–50%, 51–70% and 71–80%.

The tensile creep deformations are shown in Fig. 8 for all 10 specimens. Note that the shrinkage strain is already subtracted from the responses. The specimens that failed are indicated with a black diamond shaped marker at the point of failure.

Creep compliance is defined as the creep strain per unit stress at a specific point in time. For the further interpretation of the creep deformations, the creep compliance was calculated for each specimen at 1 min and 1.5 days respectively. The results are shown graphically in Fig. 9.

4.2. Cracking behaviour

For the representation of the statistical distribution of the cracking patterns, a skewed normal distribution was chosen. This type of distribution was chosen for its simplicity and the physicality of its parameters. It is acknowledged that a skewed normal distribution is not ideal, especially as it assumes that negative values are possible. However, it is deemed sufficient for the purpose of this paper.

A skewed normal distribution can be expressed using the average, variance and skewness of the dataset. An additional parameter is used which is not included in the statistical distribution, namely the degree of cracking which is measured as the number of cracks per metre. A typical histogram of the crack pattern of SHCC in tension together with the calculated skewed normal probability distribution function is shown in Fig. 10.

Typical SHCC crack patterns were observed for the creep specimens and an example is shown in Fig. 11. These three photos indicate the crack pattern at 1.7 days, 2.7 days and 6.9 days respectively.

The results of all the test specimens were analysed using the ARAMIS system and thereafter the distribution parameters were calculated. The average crack width, variance, skewness and degree of cracking of each specimen are shown in Figs. 12–15 respectively.

4.3. Discussion

It is clear from the tensile creep strain responses, Fig. 8, that the tensile creep increases for higher load levels. To determine whether this increase is directly proportional to the increase of the load level, the creep compliance for each specimen was calculated and is shown in Fig. 9. It seems that an increase in the creep compliance is found for higher load levels, however due to a relative large scatter and insufficient data no clear conclusion can be made.

It is however important to note that the increase of the creep strains with an increase of load level is not linear proportional to the average crack widths. It can be seen in Fig. 12 that there is a slight increase of average crack widths with an increase in load level, but not significant. Also the level of cracking, Fig. 15, indicates that the difference of the load level is not so distinguishable. It is however important to note that the variance and skewness of the

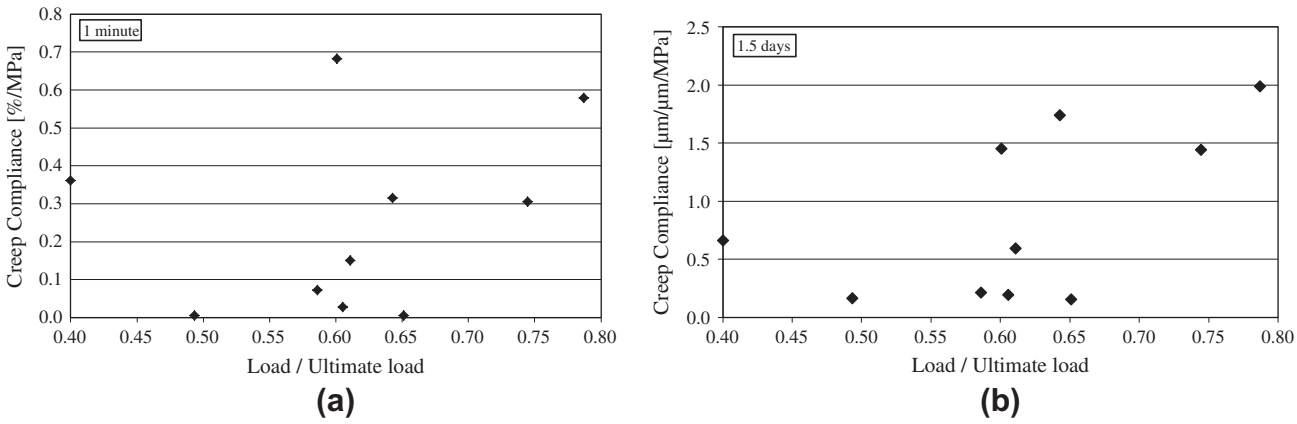

Fig. 9. Creep compliance for each load ratio at 1 min (a) and 1.5 days (b).

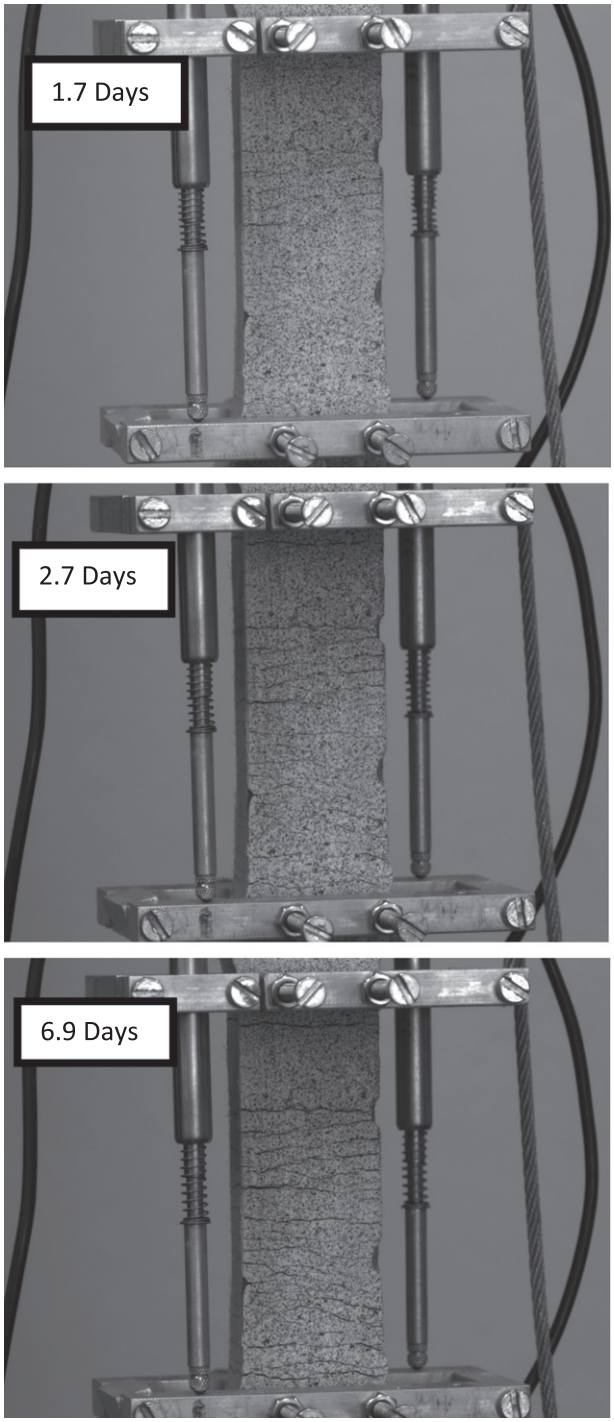

Fig. 11. Typical crack pattern observed for a creep test specimen at 1.7 days, 2.7 days and 6.9 days.

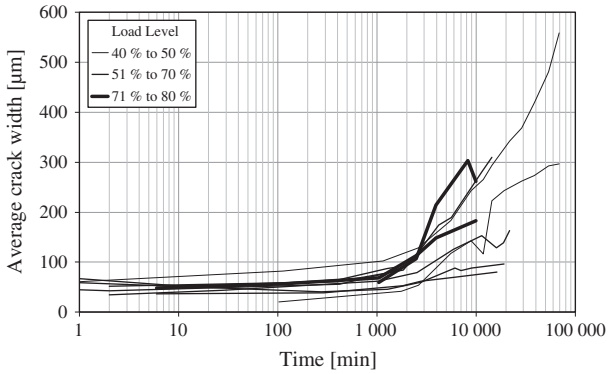

Fig. 12. Average crack width.

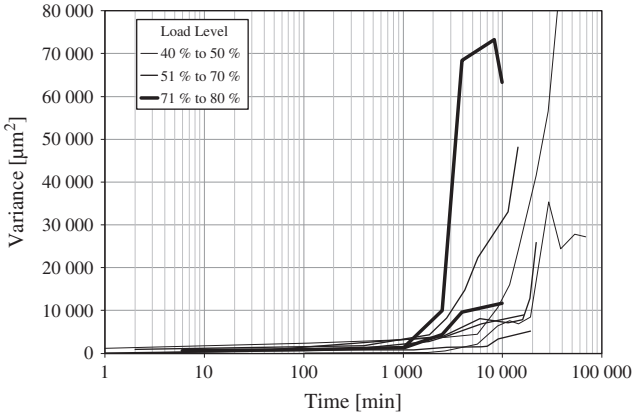

Fig. 13. Variance of the distribution of the crack widths.

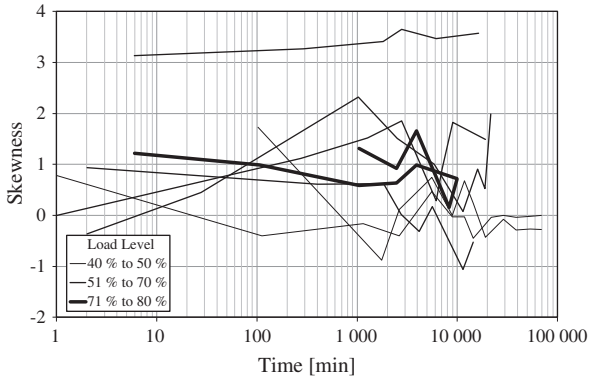

Fig. 14. Skewness of the distribution of the crack widths.

crack widths distribution, Figs. 13 and 14 respectively, seems less for lower load levels. For a lower load level the skewness values are around zero, therefore indicating a normal distribution for the crack widths, while the value increases for the higher load level tests to around 1. This indicates that for the lower loaded specimens the crack widths tends to be normally distributed whilst for the higher loaded specimens, more smaller cracks occur together with a few large cracks which is typical of a skewed normal distribution.

The strain capacity of the specimens subjected to tensile creep was in some cases more than 8% while the strain capacity of the specimens subjected to quasi-static tensile loading was not more than 5.5%. This can be contributed to the different crack patterns observed. For the quasi-static loading more cracks are found with smaller cracks widths. During the tensile creep tests, at similar strains to the quasi-static tests, there were fewer but wider cracks. Thus, even though fine, multiple, steady state cracks are observed during quasi-static loading, these crack widths increase significantly when subjected to a sustained tensile loading.

It is however concerning to note that even for the specimens that were loaded with a sustained load less than 50% of the ultimate load, the average crack widths increased above 200 µm after 7 days. The durability advantage of this material could thus be negatively influenced over time. It is however acknowledged that the

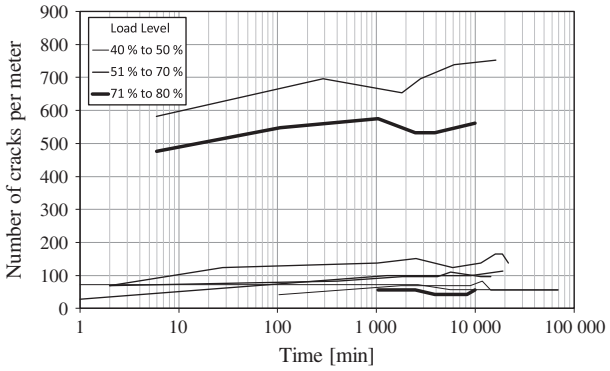

Fig. 15. Degree of cracking.

specimens are not representative of typical applications as it had no steel reinforcement. This however needs further investigation.

The creep strain responses, Fig. 8, indicates a sudden creep rate increase at after about 1200 min. It is clear from the average crack widths, Fig. 12, and the degree of cracking, Fig. 15, that this increase coincides with a crack width increase and with no significant change in the degree of cracking. This phenomenon has been reported before by Boshoff et al. [12]. The variance of the crack width distribution, Fig. 13, shows that the variance also increases significantly at this point. This clearly indicates that only a few cracks widen. It is know that the crack widths increase due to the time-dependant fibre pull-out under sustained tensile loading [11]. The mechanism responsible for this almost sudden increase of fibre pull-out rate should be further investigated.

5. Conclusions

The main objective of this research project was to quantify the cracking behaviour of SHCC under a sustained tensile load. Tensile creep loads were applied on specimens ranging from 40% to 80% of the ultimate tensile stress. The following significant conclusions can be made:

- The tensile strain of SHCC increases significantly when subjected to sustained uniaxial tensile loading.
- An increase of the sustained tensile load results in an increase of the tensile creep strain.
- The strain capacity of SHCC under sustained tensile loading is more than when subjected to quasi-static loading.
- The increase of tensile strain during creep loading is mostly attributed to crack widening which is caused by time-dependant fibre pull-out.
- After 7 days of sustained tensile loading the average crack widths can increase to more than 200 μm, even at a load less than 50% of the ultimate resistance.
- The variance of the crack width distribution increases with an increase of the creep load, however, the average crack widths seems to be almost independent of the load level between 40% and 80% of the ultimate tensile resistance.
- A sudden increase of the creep rate is found after around 1200 min and coincides with the widening of a few of the cracks and not the increase of the degree of cracking. This is caused by the time-dependant pull-out of the fibres bridging the cracks. The mechanism responsible for this almost sudden increase of pull-out rate requires further investigation.

References

[1] Boshoff WP, van Zijl GPAG. Time-dependant response of ECC: characterisation of creep and rate dependence. Cem Concr Res 2007;37:725–34.
[2] Li VC, Wang S, Wu C. Tensile strain-hardening behavior of PVA-ECC. ACI Mater J 2001;98:483–92.
[3] Maalej M, Li VC. Introduction of strain-hardening engineered cementitious composites in design of reinforced concrete flexural members for improved durability. ACI Struct J 1 1996;92:167–76.
[4] Sahmaran M, Li M, Li VC. Transport properties of engineered cementitious composites under chloride exposure. ACI Mater J 2007;104:604–11.
[5] Wang K, Jansen DC, Shah SP, Karr AF. Permeability study of cracked concrete. Cem Concr Res 1997;27:381–93.
[6] Boshoff WP, Mechtcherine V, van Zijl GPAG. Characterising the time-dependant behaviour on the single fibre level of SHCC: Part 2: the rate effects on fibre pull-out tests. Cem Concr Res 2009;39:787–97.
[7] Douglas KS, Billington SL. Rate dependencies in high-performance fibre reinforced cement-based composites for seismic application. In: Proceedings of HPFRCC conference, Hawaii; 2005.
[8] Yang E, Li VC. Rate dependence in engineered cementitious composites. In: Proceedings of HPFRCC conference, Hawaii; 2005. p. 83–92.
[9] Maalej M, Quek ST, Zhang J. Behaviour of hybrid-fibre engineered cementitious composites subjected to dynamic tensile loading a projectile impact. J Mater Civil Eng ASCE 2005;17:143–52.
[10] Rouse JM, Billington SL. Creep and shrinkage of high-performance fiber-reinforced cementitious composites. ACI Mater J 2007;104:129–36.
[11] Boshoff WP, Mechtcherine V, van Zijl GPAG. Characterising the time-dependant behaviour on the single fibre level of SHCC: Part 1: mechanism of fibre pull-out creep. Cem Concr Res 2009;39:779–86.
[12] Boshoff WP, Adendorff CJ, van Zijl WP. Creep of cracked strain hardening cement-based composites. In: Proceedings of Concreep8 conference, Japan; 2008. p. 723–8.
[13] Boshoff WP, Adendorff CJ. Modelling SHCC cracking for durability. In: Proceedings of the European conference on fracture, Dresden, Germany; 2010.
[14] Boshoff WP. Performance based approach for modelling the cracking of SHCC for durability, *fib* international workshop on performance based specifications for concrete. Leipzig: Germany; 2001.